Femtosecond interferometry of propagation of a laminar ionization front in a gas

L. A. Gizzi,[1,2] M. Galimberti,[1] A. Giulietti,[1,2] D. Giulietti,[1,2] P. Koester,[1] L. Labate,[1,2] P. Tomassini,[1,2] Ph. Martin,[3] T. Ceccotti,[3] P. De Oliveira,[3] and P. Monot[3]

[1]*Intense Laser Irradiation Laboratory, IPCF-Area della Ricerca CNR, Via Moruzzi, 1 56124 Pisa, Italy*

[2]*Istituto Nazionale di Fisica Nucleare-INFN, Pisa, Italy*

[3]*Physique à Haute Intensité, CEA-DSM/DRECAM/SPAM, Bât. 522 p. 148, 91191 Gif sur Yvette Cedex, France*

(Received 17 July 2006; published 20 September 2006)

We use optical interferometry to investigate ultrafast ionization induced by an intense, ultrashort laser pulse propagating in a helium gas. Besides standard phase shift information, our interferograms show a localized region of fringe visibility depletion (FVD) that moves along the laser propagation axis at luminal velocity. We find that such a loss of visibility can be quantitatively explained by the ultrafast change of refractive index due to the field ionization of the gas in the laser pulse width. We demonstrate that by combining the *post facto* phase shift distribution with the probe pulse transit effect in the ionizing region, the analysis of the observed FVD yields significant information on the ultrafast dynamics of propagation of the ionization front in the gas.

DOI: 10.1103/PhysRevE.74.036403 PACS number(s): 52.50.Jm, 52.25.Jm, 52.70.Kz

I. INTRODUCTION

Well-established optical interferometry techniques can provide space-resolved information at the submicrometer scale on a variety of physical systems through a measure of the phase shift induced on a probe pulse. Laser-induced plasmas are among the most common systems investigated using this technique [1]. Provided a sufficiently short probe pulse is used, evolution of plasma electron density can be followed on an ultrafast time scale using a pump and probelike approach. Similar techniques have already been successfully applied to time-resolved analysis of several phenomena including, for example, channel formation in gas jets [2], radiative blast waves [3], and characterization of plasma precursor effects in the interaction of chirped pulse amplification [4] laser pulses with solids [5]. These systems are extensively exploited for the investigation of a wide range of phenomena in both fundamental and applied sciences including the generation of ultrashort pulses of radiation from the UV [6] to the x-ray range [7], laser driven acceleration of charged particles [8] and benchmarking of high-field ionization [9] models. In this class of experiments a variety of additional optical techniques including blueshift analysis [10,11] and frequency resolved optical gating [12] are also used to acquire information on the dynamics of ionization.

The use of interferometry for the investigation of ultrafast phenomena such as ultrafast ionization of gases, can be cumbersome. In general, the transient change of the refractive index of the plasma during probe pulse duration can lead to a sizeable change of the optical path during probing, with a consequent smearing of fringes [13]. Additional complications are due to the so-called probe-transit time effect [14], that occurs when the time taken by the femtosecond probe pulse to cross the interaction region is comparable to the timescale of the process under investigation.

In this paper we report the first experiment in which optical probe interferometry has been used in a nonconventional way to detect ultrafast ionization dynamics of a gas irradiated by an intense, ultrashort chirped pulse amplification (CPA) pulse. In fact, we find that the CPA pulse induces a measurable depletion of the fringe visibility (FVD) associated with the transient change of refractive index in the ionizing region. We demonstrate that, combining this FVD with the standard phase shift information extracted at late times after pulse propagation (*post facto*) and taking into account probe-transit time in the interaction region, a quantitative investigation of the dynamics of the ionization front can be obtained. We were able to follow the ionization front from the focal region, where the intensity is well above the field ionization threshold, to the beam expanded region, where local intensity is just above the level required for a detectable ionization of the gas.

II. EXPERIMENTAL SETUP AND RESULTS

The experiment was performed at the SLIC laser facility at the Saclay Centre of CEA (France) with the 10 TW UHI10 laser system. The Ti:Sa laser system operates in the CPA mode and delivers up to 0.6 J in 60 fs laser pulses at 800 nm. The nanosecond contrast, due to the amplified spontaneous emission (ASE), was found to be $\approx 10^6$, while the picosecond *pedestal* of the femtosecond pulse had a level of $\approx 10^{-4}$ for a duration of about 1 ps before the main pulse. The main pulse was focused in the gas jet using a 200 mm, silver coated off-axis parabolic mirror. The numerical aperture of the focusing optics was $f/2.5$ and the maximum focused nominal intensity was 10^{19} W cm^{-2} in a slightly elliptical focal spot whose horizontal and vertical diameters were 8 μm and 10 μm FWHM, respectively. The corresponding normalized field parameter in the focal spot was $a_0=2.6$.

The gas jet was delivered by a 1 mm diameter, cylindrical nozzle with the laser pulse propagating at a distance of 200 μm from the tip and along a diameter of the nozzle. The He gas pressure in the valve was 8 bar resulting in a maximum neutral density around 10^{20} atoms/cm^3. The best focus was set to be at the boundary of the jet, at a sufficiently low gas density so as to prevent plasma formation by the precursor ASE radiation.

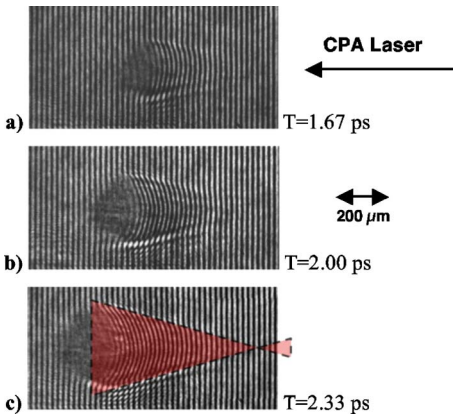

FIG. 1. (Color online) Interferogram of laser propagation in He (8 bars) taken at three different probing times as indicated in the figure. The laser pulse propagates from right to left and the dashed line in the frame (c) shows the $1/e^2$ profile of the incident beam. The localized region of transient loss of fringe visibility is clearly visible on the left, at the end of the propagation path.

A fraction of the main femtosecond pulse was frequency-doubled by a 2 mm thick, type I KDP crystal and used as an optical probe propagating perpendicular to the main pulse, in a Mach-Zehnder interferometer configuration. The probe pulse duration was estimated to be 130 fs FWHM, with a pulse shape close to a second order supergaussian profile. A test of the performance of the interferograms was carried out measuring the refractive index of neutral He gas showing that phase shift up to one tenth of a wavelength could be measured [15] from Fourier analysis [16,13] of the detected fringe pattern.

The history of the ionization of the gas was measured in a "pump and probe"-like approach, by taking a series of interferograms varying shot by shot the probe pulse-to-main pulse delay, with a time step of 330 fs. The image of Fig. 1 shows a sequence of three interferograms taken at probe times starting at 1.67 ps, where probe time zero is conventionally defined as the time at which the CPA pulse is at the position of the best focus. At these times the pulse has just passed the best focus and the fringe pattern show a conelike shape with an aperture of approximately 25°. We observe that this aperture corresponds to the full aperture of the focusing optics as indicated by the solid line that marks the $1/e^2$ profile of the beam, assuming Gaussian propagation.

The longitudinal extent of the perturbed region in the fringe pattern of Fig. 1(c) is roughly 700 μm, measured from the best focus position. This value is in a good agreement with the value expected for a propagation at the speed of light starting from the position of the best focus at probe time zero. In fact, the whole sequence of interferometric maps shows that fringe perturbation proceeds at the speed of light up to a delay time of 3 ps. Beyond that point, the position of the fringe perturbation front apparently slows down and no further propagation is detected after 3.67 ps. At this time the CPA pulse has propagated for approximately 1.2 mm beyond the best focus where the local nominal laser intensity is 1.6×10^{15} W/cm^2 and the electron density is smaller than 10^{17} cm^{-3}.

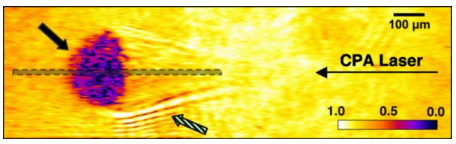

FIG. 2. (Color online) Map of fringe visibility obtained from Fourier analysis of the interferogram of Fig. 1 at 2.33 ps. The map shows a well defined region of significant loss of fringe visibility. The longitudinal lineout corresponding to the dashed region is shown in Fig. 3.

Clearly visible in the interferograms of Fig. 2 is a considerable loss of fringe visibility in an approximately elliptical region located at the leading edge of the propagating laser pulse. This feature is very reproducible and only occurs during the transit of the pulse in the region where significant ionization occurs. Also, this loss of fringe visibility is highly transient and, as discussed below, moves along with the laser pulse.

III. QUANTITATIVE ANALYSIS OF FRINGE VISIBILITY

A quantitative evaluation of FVD was obtained from our interferograms using the Fourier transform analysis applied to extract phase maps as discussed in [13]. In fact, the intensity of the fringe pattern on the detector plane (x,y) can be written as $I(x,y)=a(x,y)+[c(x,y)\exp(2\pi i f_{tr}x)+\text{c.c.}]$, where $c(x,y)=1/2b(x,y)\exp[i\Delta\varphi(x,y)]$ and its complex conjugate carry the information on phase shift $\Delta\varphi(x,y)$, background intensity $a(x,y)$, and fringe visibility $b(x,y)$. This intensity pattern can be processed using Fourier transform analysis to obtain a complex array whose imaginary part is the phase map $\Delta\varphi(x,y)$ and whose real part is the visibility of the fringes $b(x,y)$.

The image of Fig. 2 shows the visibility map of the interferogram of Fig. 1(c) as obtained from the Fourier analysis. The map is characterized by an almost flat background very close to the full visibility (100% visibility=1). As indicated by the solid block arrow, a well defined region of FVD with a characteristic asymmetric, lens-shaped profile is visible in the map. The different curvatures of the leading and trailing edges are due to the integration over the cone-shaped expanding plasma during probe transit, as explained in [14]. Some minor modulations of the fringe visibility due to diffraction of the probe beam are also visible at the lower boundary of the cone-shaped plasma as indicated by the dashed arrow. According to this map, the region of low visibility has a transverse width of 250 μm and, as shown in Fig. 3, the longitudinal depth is approximately 160 μm.

The analysis of the entire history of propagation, based upon the sequence of all interferograms and lineouts such as the one of Fig. 3, shows that a region of poor fringe visibility appears as early as probe time 1.34 ps as shown in the plot of Fig. 5. At this time the transverse size of the low visibility region is 130 μm and the longitudinal size is 70 μm. As we will show below, the observed FVD region is primarily caused by the steep ionization front propagating in the gas.

IV. LOSS OF FRINGE VISIBILITY: GENERAL PROPERTIES

We observe here that, in general, several effects may contribute to FVD in this class of measurements. In fact, de-

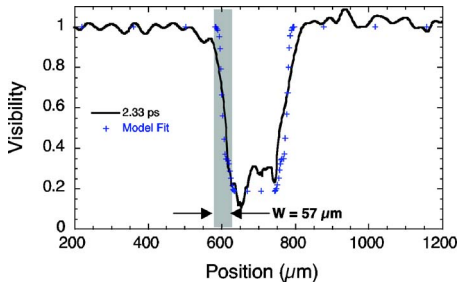

FIG. 3. (Color online) Longitudinal profile (along the laser propagation axis) of the fringe visibility taken along the dashed region of the map of Fig. 2, considering a transverse width of integration of 32 μm. The gray region identifies the width of the transition from the high to the low visibility region (see text below). The fit to the experimental data (crosses) was obtained using a model based upon propagation of a fast ionization front and taking into account the probe-transit effect (see text).

pending on the electron density distribution, the probe pulse can be partially or totally absorbed and/or deflected in the plasma. A typical feature of absorption or deflection induced FVD is its slow evolution. In fact, the density distribution will evolve on the time scale of plasma hydrodynamics and the corresponding fringe pattern will be modified on the same time-scale. Considering the plasma density and temperatures typical of our plasmas, the time scale of the hydrodynamic evolution is expected to be in the nanosecond range as observed in [13]. In contrast, the FVD observed in our measurements is highly transient and fringe visibility is fully recovered on the femtosecond time scale.

However, in the conditions investigated in our experiment, the propagating steep density gradient generated by the ionization front can still *dynamically* deflect the probe light while the probe pulse and the ionization front are crossing each other. The importance of this effect can be estimated by evaluating the deflection angle $\alpha = \ell_{pl} \nabla n / n_c$ of the probe beam propagating through the density gradient due to ionization front. Here ℓ_{pl} is the effective length over which the probe pulse experiences the gradient effect, which is basically given by the scale length of the density gradient ∇n perpendicular to the probe propagation axis. In fact, in our case, since the ionization front propagates at the speed of light, the density gradient only acts during probe transit.

To model ionization dynamics and to estimate the expected density gradient we carried out numerical simulations based on the model of ionization described in [17]. Our code calculates the rate of tunnel ionization in a nonadiabatic regime, i.e., as a function of the instantaneous laser phase, and assumes purely geometrical propagation of the beam in the plasma defined according to the real input laser parameters. The map of Fig. 4 shows a typical result of the ionization code obtained at $T = +1.8$ ps with the characteristic sharp reduction of the ionization degree visible on the left, at the position of the leading edge of the ionizing laser pulse. Similar maps taken at different times during propagation show that the depth of ionization has finite size that depends upon the local intensity and has a minimum of 10 μm at the beam waist and increases up to 40 μm at a distance of 800 μm from the best focus.

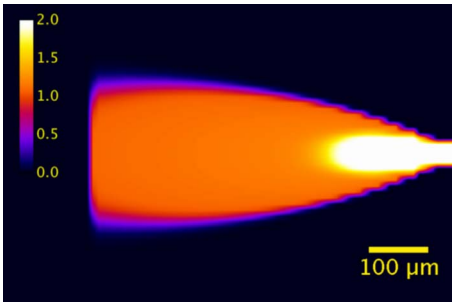

FIG. 4. (Color online) Map of the ionization degree at $T = +1.8$ ps, obtained by numerical simulation assuming tunnel ionization in a nonadiabatic regime. The map was obtained assuming geometrical propagation of the beam in the plasma defined according to the real input laser parameters.

On the basis of these result, the expected deflection of the probe beam α ranges from 10^{-3} rad at the entrance of the gas jet to 10^{-2} rad at the center of the gas jet. According to the geometry of our set up, these values of α are well within the acceptance angle of our interferometer and should not produce a significant loss of visibility.

This conclusion is further supported by the following argument. In the case of deflection, only a fraction of the probe beam reaches the image plane of the interferometer producing partial interference in the regions where absorption or deflection of the probe has taken place. In these regions, the intensity of the fringe pattern, averaged on a fringe period, should be smaller than the corresponding intensity taken on an unperturbed (no plasma) region of the interferogram. In contrast, our interferograms show that the average intensity in the FVD region is equal to the average intensity of unperturbed interferogram regions, i.e., equal to the sum of the intensities of the probe and the reference beams.

In view of the above considerations, we can restrict our analysis to the transient phase shift of the probe pulse as due to a steep ionization front propagating in the gas and try to explain the observed FVD on the basis of this mechanism. Also, as anticipated above, a correct interpretation of our results will have to include the probe transit effect that will strongly distort the way the ionization front will appear in our interferograms. In fact, our raw data show a longitudinal size of the FVD region of several hundreds of micrometers, a value much greater than the scale length of the ionization front expected according to the numerical simulations.

V. MODELING AND DISCUSSION

In general, a complex deconvolution procedure is needed to recover information on shape and size of the ionizing region from the fringe visibility map. This calculation is rather complex and is beyond the aim of the present paper. Here we use a simple model based upon integration of the time dependent phase shift as discussed in [14] to estimate the expected FVD and to demonstrate that our technique based on a quantitative evaluation of the FVD can provide access to information on the transient ultrafast ionization.

Lineouts similar to the one of Fig. 3 for all visibility maps show that the loss of visibility at a given probe time, exhibits

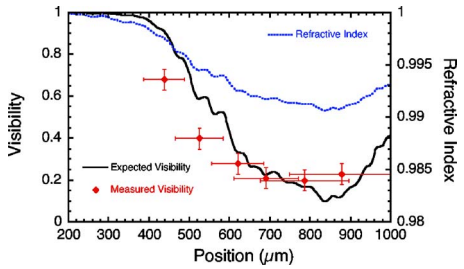

FIG. 5. (Color online) Measured history (diamonds) of the fringe visibility at six probing times starting from +1.34 ps every 330 fs. The value at each probing time was taken from the average of the FVD region similar to the one visible in Fig. 2 (bottom) over a 32 μm transverse width. Also visible in the plot is the expected fringe visibility (solid curve) calculated (see text) from Eq. (1) using the experimental profile of the *post facto* refractive index on axis (dashed curve). The laser propagates from left to right.

an almost flat-top profile with a top level decreasing gradually from approximately 70% to approximately 20% loss with respect to the unperturbed visibility value as shown in the plot of Fig. 5. Also, the FWHM of each curve increases from approximately 100 μm at 1.34 ps to more than 250 μm at 3 ps. At times later than 3 ps visibility is rapidly restored and at probe time +4.67 ps almost full recovery of fringes occurs. Beyond this time, interferograms show a clear fringe pattern varying very slowly on a *ns* time scale.

A quantitative analysis of the observed fringe visibility depletion can be carried out assuming that $c\tau+\Delta$ is smaller than the longitudinal extent of the region of FVD, where τ is the probe pulse duration, c is the speed of light, and Δ is the longitudinal size of the ionization front propagating in the gas. According to the results of the simulations given above, this condition is well satisfied in our experiment. In these circumstances, it is possible, in principle, to carry out exact calculations that accounts for the finite depth of the ionization to yield the value of this depth.

A brief introduction to the modeling of interferograms discussed in [14] is given below, focused on the main expected features concerning fringe visibility. Assuming that the probe pulse is propagating perpendicular to the pump (ionizing) pulse, the signal S at the detector plane (y,z) of the interferometer can be written as

$$S(y,z,T) = \int_{-\infty}^{+\infty} I_p(t)[1 + V_0\cos(\Phi(y,z,T+t) + 2\pi z/\lambda_p)]dt,$$

where I_p is the probe pulse intensity, Φ is the phase shift on the probe pulse, and T is the probing time (delay) conventionally set to zero when probe and pump pulses cross each other at $y=z=0$. The evaluation of this expression in our experimental conditions as discussed above shows that a nearly flat-top region of FVD is expected with the value of visibility given by

$$V = V_o\left|\frac{\sin(A)}{A}\right|, \qquad (1)$$

where $A=\pi\delta\mu c\tau/\lambda_p$, $\delta\mu$ is the change of refractive index during ionization and λ_p is the probe pulse wavelength. This relationship accounts for the loss of visibility due to the change of the refractive index experienced by the probe pulse during transit in the ionizing region, due to its finite duration. In other words, as the refractive index of the probed region changes while the probe pulse is crossing it, the instantaneous phase shift induced on the probe pulse also changes with a consequent shift of the instantaneous fringe pattern at the detector plane. Since the signal on the detector is time integrated over the entire probe pulse duration, the final result will be the integration of a moving pattern of fringes, i.e., a "smeared" fringe pattern. According to Eq. (1), as the change of refractive index increases, the visibility exhibits a heavily damped oscillation going to zero when the optical path is a multiple integer of the probe wavelength. This behavior also implies that the best operating conditions for this analysis to work can be achieved when $A<\pi$. In this parameter range, the maximum phase shift change of the probe pulse corresponds to less than a probe wavelength and, according to Eq. (1), the visibility is a unique and monotone function of A. As shown below, this is also the case of the experiment presented here.

In fact, in our case, the local change of refractive index can be calculated as the difference between the refractive index of the ionized gas (measured immediately after pump pulse propagation) and the refractive index of the neutral He gas. The refractive index obtained from the experimental density profile of Fig. 5 (dashed line) is then used to calculate the fringe visibility curve expected according to Eq. (1). The final result is plotted in Fig. 5 and is compared with the measured values of FVD (diamonds). According to this plot, the measured maximum FVD is found to be in a good agreement with the value expected according to the simple model. Some discrepancy is found in the temporal evolution of expected and measured value of the fringe visibility that may be partially due to the square probe pulse profile used in our model. Also, some temporal uncertainty may arise from the actual duration of the probe pulse in comparison with the nominal value used in our calculations. According to our estimates, this may account for relatively small changes of the expected visibility that may explain the discrepancy between measured and expected history of FVD.

A straightforward result of this comparison is that the value of the flat-top FVD observed in our experiment, can be quantitatively explained according to Eq. (1) by taking into account the transient change of refractive index induced by a CPA pulse propagating in a He gas. Indeed, the visibility map of Fig. 2 can be further analyzed to provide information on Δ, i.e., the depth of the ionization front. In fact, according to our model [14], the width of the transition from the low visibility to the high visibility region marked by the gray area of Fig. 3 is simply given by $c\tau+\Delta$. Therefore, the depth of the ionization front can be immediately derived by the longitudinal extent of the transition region.

As an example, in the case of the visibility map at 2.33 ps, the transition region is approximately 57 μm. Taking into account the probe pulse duration of 130 fs, the above relationship yields $\Delta \approx 18$ μm. Alternatively, the value of Δ can be obtained by fitting the whole visibility curve of Fig. 3 with the calculated curve as obtained from the model. The plot of Fig. 3 shows the best fit (crosses) to the visibility

curve that yields $\Delta \approx 17.5$ μm. Both these values are fully consistent with each other and provide a significant piece of quantitative information on the physical process under investigation. It is interesting to compare this value with the value of the depth of the ionization front given by our ionization code as described above. According to our simulations, at the time of 2.33 ps the depth of ionization is found to be approximately 30 μm, a value which is significantly greater than the one observed experimentally. This discrepancy is most likely due to partial description of beam propagation physics included in the code, that leads to an underestimation of the laser intensity, with a consequent increase of the depth of ionization. Although more work is needed to fully address this issue, at this stage however, we can already conclude that the quantitative information obtained with our measurements provide an observation of the propagation of a thin ionization slab in the gas and demonstrates the effectiveness of our original probing technique that combines the traditional fringe pattern analysis of the *post facto* (after propagation) density map, with the loss of fringe visibility inherent with the *live* (during propagation) probing analysis.

Moreover, our findings show that our technique has the potential for detecting fast ionization dynamics with very high temporal and spatial resolution. In fact, as pointed out above, the length of the probe pulse plays a critical role in defining the final spatial resolution of this measurement. The use of a few-cycle probe pulse could, in principle, enable the investigation of the ionization region at the μm scale, a level sufficient to explore the spatiotemporal structure of the ionization front produced in the case of gases with a higher atomic number. The use of a very short probe pulse in the class of experiments discussed here may also enable measurements of the depth of ionization front with the level of accuracy required for benchmarking of ionization codes.

VI. CONCLUSIONS

We have presented experimental results concerning the propagation of an intense, ultrafast laser pulse in a helium gas jet. Our high quality, time resolved interferometric probe enabled us to detect a thin slab of ionization induced by the CPA pulse propagating in the gas. The loss of visibility of interferometric fringes, combined with probe transit effect analysis, was successfully used for the first time to track down the propagation of the ionization front in the gas. Our measurements show that ionization occurs in a very thin layer that propagates in the gas at the speed of light.

ACKNOWLEDGMENTS

We would like to thank the staff of the SLIC laser facility for their invaluable and friendly support. We acknowledge support from the LASERLAB EUROPE Trans-national Access Programme. We thank A. Barbini, W. Baldeschi, and M. Voliani of the IPCF staff for their invaluable technical assistance. This work was partially supported by the joint INFN-CNR Project "Plasmon-X" and by the MIUR funded CNR project "Impianti Innovativi Multiscopo per la Produzione di radiazione X e Ultravioletta."

[1] O. Willi, in *Laser-Plasma Interactions 4, Proceedings of the XXXV SUSSP, St. Andrews, 1988*, edited by M. B. Hooper (SUSSP, Edinburgh, 1989).
[2] M. Dunne, T. Afshar-Rad, J. Edwards, A. J. MacKinnon, S. M. Viana, O. Willi, and G. Pert, Phys. Rev. Lett. **72**, 1024 (1994); V. Malka *et al.*, Phys. Rev. Lett. **79**, 2979 (1997).
[3] M. J. Edwards, A. J. MacKinnon, J. Zweiback, K. Shigemori, D. Ryutov, A. M. Rubenchik, K. A. Keilty, E. Liang, B. A. Remington, and T. Ditmire, Phys. Rev. Lett. **87**, 085004 (2001).
[4] D. Strickland and G. Mourou, Opt. Commun. **56**, 219 (1985).
[5] D. Giulietti *et al.*, Phys. Plasmas **9**, 3655 (2002).
[6] Y. Mairesse *et al.*, Phys. Rev. Lett. **93**, 163901 (2004).
[7] A. Rousse *et al.*, Phys. Rev. Lett. **93**, 135005 (2004).
[8] S. P. D. Mangles *et al.*, Nature (London) **431**, 535 (2004); C. G. R. Geddes *et al.*, *ibid.* **431**, 538 (2004); J. Faure *et al.*, Nature (London) **431**, 541 (2004).
[9] B. Walker, B. Sheehy, L. F. DiMauro, P. Agostini, K. J. Schafer, and K. C. Kulander, Phys. Rev. Lett. **73**, 1227 (1994).
[10] D. Giulietti, L. A. Gizzi, A. Giulietti, A. Macchi, D. Teychenne, P. Chessa, A. Rousse, G. Cheriaux, J. P. Chambaret, and G. Darpentigny, Phys. Rev. Lett. **79**, 3194 (1997).
[11] C. W. Siders *et al.*, J. Opt. Soc. Am. B **13**, 300 (1996).
[12] C. W. Siders, G. Rodriguez, J. L. W. Siders, F. G. Omenetto, and A. J. Taylor, Phys. Rev. Lett. **87**, 263002 (2001).
[13] L. A. Gizzi, D. Giulietti, A. Giulietti, T. Afshar-Rad, V. Biancalana, P. Chessa, C. Danson, E. Schifano, S. M. Viana, and O. Willi, Phys. Rev. E **49**, 5628 (1994); M. Borghesi, A. Giulietti, D. Giulietti, L. A. Gizzi, A. Macchi, and O. Willi, *ibid.* **54**, 6769 (1996).
[14] M. Galimberti, J. Op. Soc. Am. A (to be published); M. Galimberti, IPCF-CNR Internal Report, 1032005 (2005).
[15] L. A. Gizzi *et al.*, Proceedings of the 3rd International Conference on Superstrong Fields in Plasmas, *AIP Conf. Proc.* Vol., 827, 3 edited by M. Lontano *et al.* (AIP, Melville, N.Y., 2006).
[16] M. Takeda, H. Ia, and S. Kobayashi, J. Opt. Soc. Am. **72**, 156 (1982).
[17] G. L. Yudin and M. Y. Ivanov, Phys. Rev. A **64**, 013409 (2001).